Critical Phenomenon Analysis of Shear-Banding Flow in Polymer-like Micellar Solutions. 1. Theoretical Approach

Fernando Bautista,*,† Manuel Muñoz,‡ Jorge Castillo-Tejas,§ Juan H. Pérez-López,‡ Jorge E. Puig,‡ and Octavio Manero||

Departamentos de Física e Ingeniería Química, Universidad de Guadalajara, Boul. M. García-Barragán # 1451 Guadalajara, Jal. 44430, Mexico, Facultad de Ciencias Básicas, Ingeniería y Tecnología, Universidad Autónoma de Tlaxcala, Calz. Apizaquito S/N, Apizaco, Tlax. 90300, México, and Instituto de Investigaciones en Materiales, Universidad Nacional Autónoma de México, Apdo. Postal México, D.F. 04510, México

Received: July 3, 2009; Revised Manuscript Received: September 14, 2009

The shear-banding flow in polymer-like micellar solutions is examined here with the generalized Bautista−Manero−Puig model. The coupling between flow and diffusion naturally arises in this model, which is derived from the extended irreversible thermodynamic formalism. The limit of an abrupt interface is treated here. The model predicts a dynamic master steady-flow diagram, in which all data collapse at low shear rates. Moreover, the model predicts that a nonequilibrium critical line is reached upon decreasing the shear-banding intensity parameter of the model, which corresponds to increasing temperature, increasing surfactant concentration, or varying salt-to-surfactant concentration ratio. By employing nonequilibrium critical theory and the concept of dissipated energy (or extended Gibbs free energy), a set of symmetrical reduced stress versus reduced shear-rate curves are obtained similar to gas−liquid transitions around the critical point. In addition, the nonequilibrium critical exponents are derived, which follow the extended Widom's rule and the extended Rushbroke relationship, but they are nonclassical.

Introduction

The description of nonequilibrium systems has been a standing problem for the fundamental understanding of the behavior of complex fluids. The features generally observed in equilibrium systems close to a phase transition, such as universality and scale invariance, can also arise from nonequilibrium dynamics.[1] A straightforward approach to describe nonequilibrium systems is seeking similar methods or theories used in equilibrium critical behavior.

Nonequilibrium systems can be classified into two main groups: those that are driven and evolve to a steady state but never reach equilibrium, and those that relax to a final equilibrium state. In complex fluids, such as micellar solutions, block copolymers, associative polymers, and so on, both behaviors are observed.[2] Elsewhere it has been shown that along the region bounded by two critical shear rates ($\dot{\gamma}_{c1}$ and $\dot{\gamma}_{c2}$) where a stress plateau develops and shear-banding flow arises, dynamic equilibrium (in this case, a steady flow) in some systems is not achieved, and stress oscillations that last very long times upon inception of shear flow are observed.[3−8] Indeed, the constitutive response is intrinsically unsteady in some regimes.[9] An opposite situation is detected along the regions where the flow is stable and the solution tends to a definite steady state. Examples of the former class that exhibit critical behavior are systems that undergo a nonequilibrium phase transition. This kind of shear-induced phase transition as well as nonequilibrium critical points (necp) have been examined both theoretically and experimentally in complex fluids such as polymers[2,10−12] and micellar solutions.[13−20]

Optical and small-angle neutron scattering (SANS) measurements have examined the alignment of micellar solutions under flow. Early optical experiments on wormlike micelles show a temporally oscillating state with alternating turbid and clear bands.[21] Indeed, along the stress plateau region, turbidity and flow dichroism arise. SANS measurements have shown that the turbid band has higher alignment than the isotropic band.[21,22] This observation is explained to be due to shear bands composed of a highly branched concentrated micellar solution coexisting with an isotropic phase. The shear banding observed is proposed to be connected with an underlying thermodynamic phase separation.

For wormlike micellar solutions, the intrinsic constitutive curve of shear stress as a function of shear rate may be nonmonotonic. The constitutive curve has a maximum in the stress and a region of decreasing stress where steady homogeneous flow is unstable. Several models predict that the system must separate into low- and high-shear-rate bands for applied shear rates in the unstable region of the constitutive curve.[17,23−25] Experimentally, for shear-thinning wormlike micelles, the steady-state flow curve has a well-defined and reproducible plateau.[18,19,26] The stress selection problem has been addressed in various analyses. One of them includes interfacial gradient terms into the constitutive equation and predicts a diffusion of the stationary front between the low- and high-shear-rate bands.[18] The former descriptions that consider coupling flow and diffusion have been undoubtedly useful and have led to a considerable amount of scientific work.[13,14,17] However, this approach presents some drawbacks from the fundamental points of view, because it is based on the inclusion of ad hoc terms. It is conceivable, indeed, that other variables not found in equilibrium may influence the thermodynamic equations in nonequilibrium situations, as in the extended irreversible thermodynamic (EIT) formalism. Our approach considers the

* Corresponding author. E-mail: ferbautistay@yahoo.com.
† Departamento de Física, Universidad de Guadalajara.
‡ Departamento de Ingeniería Química, Universidad de Guadalajara.
§ Universidad Autónoma de Tlaxcala.
|| Universidad Nacional Autónoma de México.

10.1021/jp906310k CCC: $40.75
Published on Web 11/19/2009

coincidence of the minimum in the dissipation energy (or extended Gibbs free energy) of the two relevant stable branches to set the position of the stress plateau,[9] which is in agreement with the equal-areas criterion.

As shown elsewhere,[9,25] the constitutive flow curve of the Bautista−Manero−Puig (BMP) model strongly resembles the pressure−volume ($P-V$) plot as a function of temperature predicted by the van der Waals or other cubic equation of state.[27] The constitutive flow curve exhibits a coexistence (of bands) envelope, a region of instability akin to the spinodal region in $P-V$ plots, and two metastable regions that collapse into a "critical" or inflection point. In fact, as observed experimentally, when the temperature or the surfactant concentration is increased, the shear-banding flow region diminishes, and it vanishes at a critical temperature or surfactant concentration, defining a critical line (or surface when an extra component such as a salt is added), inasmuch as polymer-like micellar solutions are two- or three-component systems.[8,28,29]

According to the usual description of critical phenomena and assuming that the scaling laws for equilibrium and nonequilibrium critical transitions have the same mathematical form,[30,31] the dominant part of the functions that describe the system properties near the critical point should be mathematically simple, since a system is very insensitive to the details of its dynamics or structure near critical points. Then equilibrium (and perhaps, nonequilibrium) systems near a critical point obey a series of power laws with various exponents, called *critical exponents*, which can be measured experimentally.[30,31]

The classical critical exponents describe how various singular quantities, such as the order parameter and the specific heat, depend on the difference between the current and critical temperatures.[30,31] An analogous order parameter in nonequilibrium critical behavior might be the time t,[32] or its reciprocal, the shear rate for a flowing system, $\dot{\gamma}$. For shear-banding flow, *here it is proposed* that an appropriate order parameter could be the difference between the shear rates, $\dot{\gamma}$ and $\dot{\gamma}_{c1}$. This is based on the fact that this difference characterizes the degree of order in the system because it corresponds to the departure between homogeneous and nonhomogeneous flows, as shown elsewhere.[9,28] In addition, it is a fluctuating scalar field of order unity upon renormalization that exhibits a discontinuity at the transition point for a nonequilibrium first-order phase transition. This choice is analogous to a real gas order parameter and follows all the characteristics of the equilibrium order parameters. In this regard, the order parameter for shear-banding flow may be given by $\phi = \dot{\gamma}(y) - \dot{\gamma}_{c1}(y)$, where y is velocity gradient direction.

In this work, the first of two articles, the generalized Bautista−Manero−Puig model is used to analyze the nonequilibrium critical phenomenon in wormlike micellar solutions that exhibit shear-banding flow. This model predicts the *master dynamic flow diagram* proposed by Berret et al.[29] and the existence of a critical line as the shear-banding intensity parameter of this model—which corresponds to increasing temperature, surfactant concentration, or varying salt-to-surfactant concentration ratio—goes to zero. The model also predicts that in the shear-banding flow region coexist at least two different bands that dissipate equal power; i.e., the shear-banding flow is a first-order nonequilibrium phase transition. Additionally, the model demonstrates that the nonequilibrium critical exponents follow the extended Widom's rule and the extended Rushbroke inequality. Nevertheless, they are nonclassical. The model predictions are in agreement with the scaling hypothesis. In part 2, experimental evidence is provided in several micellar solutions that exhibit shear-banding flow, supporting the existence of a nonequilibrium critical point in these systems.

Theoretical Section

Extended irreversible thermodynamics provides a consistent form to derive constitutive equations for systems far from equilibrium. Beyond the local equilibrium hypothesis, EIT assumes the existence of a regular and continuous function η_E that plays the role of generalized entropy and considers independent variables such as the dissipative fluxes in addition to the classical variables, i.e., internal energy, density, etc.[33] The fluid is assumed to be incompressible, heat-insulated with constant internal energy, and chemically inert.

The Generalized BMP Model and the Master Flow Diagram. The set of equations of the generalized BMP model are[34]

$$\frac{d\varphi}{dt} = \frac{1}{\lambda}(\varphi_0 - \varphi) + k_0(1 + \vartheta\Pi_D)(\varphi_\infty - \varphi)\underline{\sigma}:\underline{D} + \varphi_0\beta'_0\nabla\cdot\bar{J} \quad (1)$$

$$\bar{J} + \tau_1\frac{\varphi_0}{\varphi}\overset{\nabla}{\bar{J}} = -\frac{D\varphi_0}{\varphi}\nabla c - \frac{\beta_0}{\varphi}\nabla\varphi + \frac{\beta_2\varphi_0}{\varphi}\nabla\cdot\underline{\sigma} \quad (2)$$

$$\underline{\sigma} + \frac{1}{G_0\varphi}\overset{\nabla}{\underline{\sigma}} = \frac{2}{\varphi}\underline{D} + \frac{\beta_2'\varphi_0}{\varphi}\nabla\bar{J} \quad (3)$$

where the upper-convected derivatives of the mass flux vector $\bar{J}$ and of the stress tensor $\underline{\sigma}$ are defined, respectively, as

$$\overset{\nabla}{\bar{J}} = \frac{d\bar{J}}{dt} - \underline{L}\cdot\bar{J} \quad (4)$$

$$\overset{\nabla}{\underline{\sigma}} = \frac{d\underline{\sigma}}{dt} - (\underline{L}\cdot\underline{\sigma} + \underline{\sigma}\cdot\underline{L}^T) \quad (5)$$

Here $\underline{L}$ is the velocity gradient tensor, $\underline{D}$ is the symmetric part of rate of strain tensor and II_D is its second invariant, φ is the inverse of the shear viscosity (η) or fluidity, φ_0 ($\equiv\eta_0^{-1}$) is the fluidity at zero shear rate, G_0 is the plateau shear modulus, λ is a structure relaxation time, k_0 can be interpreted as a kinetic parameter for structure breaking under shear flow, τ_1 is a relaxation time for the mass flux, D is the Fickean diffusion coefficient, c is the local equilibrium concentration, and ϑ, β_0, β_0', β_2 and β_2' are phenomenological parameters.

Equations 1−3 together with the conservation equations represent a closed set of time evolution equations for all the independent variables chosen to describe the behavior of complex fluids. The relaxation equations for the nonconserved variables have been obtained considering only restricted second-order terms in the constitutive variables (φ, $\bar{J}$, $\underline{\sigma}$) and up to first-order terms in $\underline{L}$. Note that these equations are double-coupled to each other: eq 1 contains a coupling of the structure parameter and the stress tensor; eq 2 has a coupling of the mass flux and the structure parameter; and eq 3 involves the coupling of the stress tensor and the mass flux.

Normal stresses are not included in eqs 1−3, since their contribution does not change qualitatively the results of the critical analysis that follows. Notwithstanding, their effects are considered and discussed below. Solutions to eqs 1−3, in which

the coupling coefficients are nonzero, predict shear bands, rheochaos, and a rich rheological behavior.[35] In addition, a theoretical analysis on the effect of shear on the microstructural order and shear-induced structure formation, which plays an important role in shear banding, can be found in a recent paper.[36] In this analysis, the flow−concentration coupling is considered in a model that theoretically explains the experimentally observed instabilities in shear-thinning and shear-thickening complex fluids. These instabilities may occur along the gradient and vorticity axes. In addition, it shows that due to the flow−concentration coupling, the regions of instability broaden to include regions of positive slope in the constitutive flow curve and that the critical point shifts downward.

For steady simple shear, assuming that the gradients in φ and c vary along the y-direction, and after neglecting the relaxation time for the mass flux, eqs 1−3 become

$$\frac{1}{\lambda}(\varphi_0 - \varphi) + k_0(1 + \vartheta\Pi_D)(\varphi_\infty - \varphi)\sigma\dot{\gamma} + \varphi_0\beta_0'\frac{\partial J_y}{\partial y} = 0 \quad (6)$$

$$J_x = \frac{\beta_2\varphi_0}{\varphi}\frac{\partial\sigma}{\partial y},\ J_y = -\frac{D\varphi_0}{\varphi}\frac{\partial c}{\partial y} - \frac{\beta_0}{\varphi}\frac{\partial\varphi}{\partial y} \quad (7a, 7b)$$

$$\sigma = \frac{\dot{\gamma}}{\varphi} + \frac{\beta_2'\varphi_0}{\varphi}\frac{\partial J_x}{\partial y} \quad (8)$$

In eqs 7a and 7b we have assumed that normal stresses are negligible. Equations 6−8 embody particular cases. For instance, substituting eq 7b into eq 6 for the case where differences in concentration are negligible yields

$$\frac{1}{\lambda}(\varphi_0 - \varphi) + k_0(1 + \vartheta\dot{\gamma})(\varphi_\infty - \varphi)\sigma\dot{\gamma} - \varphi_0\beta_0\beta_0'\frac{\partial}{\partial y}\left(\frac{1}{\varphi}\frac{\partial\varphi}{\partial y}\right) = 0 \quad (9)$$

Equation 9 is a reaction-diffusion-like equation similar to that analyzed by Pearson[37] and Goveas et al.[38] The diffusion term in this equation is the analog of the nonlocal terms in the free energy equation and provides gradients that can support inhomogeneities and describe interfaces between states. According to Goveas and Olmsted,[38] this term is supposed to be necessary for determining the conditions of phase coexistence under flow. The magnitude of the coefficient of this term is proportional to the magnitude of the interfacial width.

On the other hand, when eq 7a is substituted in eq 8 gives

$$\sigma = \frac{\dot{\gamma}}{\varphi} + \frac{\beta_2\beta_2'\varphi_0^2}{\varphi}\frac{\partial}{\partial y}\left[\frac{1}{\varphi}\frac{\partial\sigma}{\partial y}\right] \quad (10)$$

Equation 10 now contains diffusion terms for the stress. The inclusion of these nonlocal terms in the constitutive equation has been invoked elsewhere to resolve the location of the plateau stress.[39−43] Furthermore, the EIT formulation also provides a coupling between eqs 9 and 10, inasmuch as the solution for φ in eq 9 is used to obtain the stress in eq 10. Yuan and Jupp[40] pointed out, on the basis of a coupling of stress with diffusion, that there is no need to introduce any ad hoc diffusive stress term into the constitutive equations as in earlier studies of shear banding.[41−43] The steady-state stress for nonmonotonic constitutive equations can be selected by the coupled model. Consequently, a coupling between viscoelasticity and diffusion, which naturally arises in the EIT formulation, provides the gradient terms more consistently for the stress selection as it has been shown by us elsewhere.[28,34] With regard to the shear-banding state, a banding solution (homogeneous phases separated by an interface) is, by definition, one that has no gradients of φ at the boundaries. At the conditions where the phase coexistence is present, the fluidity is constant within the bulk of each phase. Fluidity changes suddenly at the interface, wherein it is assumed that

$$\frac{\partial\varphi}{\partial y} = \delta(y - y_I) \quad \text{or} \quad J_y = \frac{\beta_0}{\varphi}\Big|_{y=y_I} = \frac{\beta_0}{\varphi(\dot{\gamma}_{c1})} \quad (11)$$

and similarly for J_x. Hence, eqs 6 and 8 become

$$\frac{1}{\tau_0}(\varphi_0 - \varphi) + k_0(1 + \vartheta\dot{\gamma})(\varphi_\infty - \varphi)\sigma\dot{\gamma} = 0 \quad (12)$$

$$\sigma = \frac{\dot{\gamma}}{\varphi} \quad (13)$$

and they reduce to the nondiffusive equations for simple steady shear. Integrating eq 8 gives

$$\frac{1}{\beta_2'\varphi_0}\int_{\dot{\gamma}_{C1}}^{\dot{\gamma}_{C2}}(\sigma\varphi - \dot{\gamma})d\dot{\gamma} = 0 \quad (14)$$

where $\dot{\gamma}_{C1}$ and $\dot{\gamma}_{C2}$ are the critical shear rates that signal the onset and end of the stress plateau. The result in eq 14 has been termed by Dhont[44] as the "modified Maxwell equal-area construction".

At this point, it is important to address the fact that eq 14 is of fundamental importance for the selection of the plateau stress and the critical shear rates. The fact is that at the critical shear rates, the shear-rate gradients vanish since the strain rate here is independent of position. Since the coexistence curve depends on the difference of these two critical shear rates, this curve is independent of the gradient terms, and therefore, the integral in eq 14, and hence the dissipated energy, is also independent of the coordinates. This means that the dissipated energy does not change if gradient terms are included.

In this regard, in the limit of an abrupt interface, the time-dependent equations read

$$\frac{d\varphi}{dt} = \frac{1}{\lambda}(\varphi_0 - \varphi) + k_0(1 + \vartheta\dot{\gamma})(\varphi_\infty - \varphi)\sigma\dot{\gamma} \quad (15)$$

$$\sigma + \frac{1}{G_0\varphi}\frac{d\sigma}{dt} = \frac{\dot{\gamma}}{\varphi} \quad (16)$$

In these equations, σ and $\dot{\gamma}$ are the shear stress and shear rate, respectively, and ϑ is the shear-banding intensity parameter, which, as shown elsewhere,[9,28] is related to the stress plateau selection by the modified Maxwell equal-area construction.

Substitution of eq 16 into eq 15 yields an equation that can be expressed in terms of the dimensionless variables proposed by Berret et al.,[29] mainly, $\hat{\sigma} = \sigma/G_0$, $\hat{\dot{\gamma}} = \dot{\gamma}\,\tau_R$, and $\hat{t} = t/\tau_R$

$$\frac{1}{\hat{\sigma}}\left(\frac{d\hat{\sigma}}{d\hat{t}}\right)^2 - \frac{d^2\hat{\sigma}}{d\hat{t}^2} - \left[\frac{\hat{\dot{\gamma}}}{\hat{\sigma}} + \frac{1}{\hat{\lambda}} + \mathbf{k}_0(1 + \hat{\vartheta}\hat{\dot{\gamma}})\hat{\sigma}\hat{\dot{\gamma}}\right]\left(\frac{d\hat{\sigma}}{d\hat{t}}\right) = \frac{(\hat{\sigma} - \hat{\dot{\gamma}})}{\hat{\lambda}} + \mathbf{k}_0(1 + \hat{\vartheta}\hat{\dot{\gamma}})(\hat{\sigma}\hat{\varphi}_\infty - \hat{\dot{\gamma}})\hat{\sigma}\hat{\dot{\gamma}} \quad (17)$$

where $\mathbf{k}_0 = G_0 k_0$, $\hat{\lambda} = \lambda/\tau_R$, $\hat{\vartheta} = \vartheta/\tau_R$, and $\hat{\varphi}_\infty = G_0\tau_R\varphi_\infty = \varphi_\infty/\varphi_0$. This equation contains four dimensionless parameters $\hat{\lambda}$, $\mathbf{k}_0$, $\hat{\vartheta}$ and $\hat{\varphi}_\infty$, and two independent variables, either $\hat{\sigma}$ or $\hat{\dot{\gamma}}$ and $\hat{t}$. Under steady state (or dynamic equilibrium), which is the situation examined here, the left-hand side of eq 17 becomes zero and reduces to the following dimensionless cubic equation in shear rate. In order to simplify the nomenclature, we drop the superscript (ˆ) such as $\hat{\lambda} = \lambda$, $\hat{\vartheta} = \vartheta$, $\hat{\varphi}_\infty = \varphi_\infty$, $\hat{\sigma} = \sigma$, $\hat{\dot{\gamma}} = \dot{\gamma}$ and $\hat{t} = t$

$$\dot{\gamma}^3 + \left(-\varphi_\infty\sigma + \frac{1}{\vartheta}\right)\dot{\gamma}^2 + \left(-\frac{\varphi_\infty}{\vartheta}\sigma + \frac{1}{k\vartheta\sigma}\right)\dot{\gamma} - \frac{1}{k\vartheta} = 0 \quad (18)$$

where $k = \mathbf{k}_0\lambda$. For steady state the number of constants reduce to three, k, ϑ and φ_∞, and one independent variable, either σ or $\dot{\gamma}$. For very small shear rates, the quadratic and cubic terms may be neglected, and so $\sigma = \dot{\gamma}$, which indicates that the predicted data collapse in a single line with slope equal to one at low shear rates. Hence, the dimensionless BMP equation predicts the normalization suggested by Berret et al.,[29] as it will be shown in the Results and Discussion section.

Locus of the Critical Point and Its Dependence on the Dimensionless Model Parameters. At the nonequilibrium critical point (necp), the three roots of eq 18 are equal. Hence, this equation can be rewritten as

$$(\dot{\gamma} - \dot{\gamma}_c)^3 = \dot{\gamma}^3 - 3\dot{\gamma}^2\dot{\gamma}_c + 3\dot{\gamma}\dot{\gamma}_c^2 - \dot{\gamma}_c^3 = 0 \quad (19)$$

which yields

$$\dot{\gamma}_c = \dot{\gamma}_1 = \dot{\gamma}_2 = \dot{\gamma}_3 = -\frac{1}{3}\left(\frac{1}{\vartheta_c} - \varphi_\infty\sigma_c\right) = \sqrt{\frac{1 - k\varphi_\infty\sigma_c^2}{3k\vartheta_c\sigma_c}} = \frac{1}{(k\vartheta_c)^{1/3}} \quad (20)$$

The stress and fluidity at the critical point are given by

$$\sigma_c = \frac{1}{\vartheta_c\varphi_\infty} + \frac{3}{\varphi_\infty(k\vartheta_c)^{1/3}} = \frac{1}{\vartheta_c\varphi_\infty}\left(1 + \frac{3\vartheta_c^{2/3}}{k^{1/3}}\right) \quad (21)$$

$$\varphi_c = \frac{\varphi_\infty\vartheta_c}{3\vartheta_c + (k\vartheta_c)^{1/3}} \quad (22)$$

In order to find a relationship among the model parameters, the expression $((1 - k\varphi_\infty\sigma_c^2)/(3k\vartheta_c\sigma_c))^{1/2} = 1/((k\vartheta_c)^{1/3})$ is chosen, and upon defining two new parameters, $\xi = \vartheta_c^{2/3}$ and $\zeta = k^{-1/3}$, it is found after straightforward algebraic work that

$$(\varphi_\infty - 9)\xi^3 - 12\xi^2\zeta - 6\xi\zeta^2 - \zeta^3 = 0 \quad (23)$$

This equation suggests that only two dimensionless model parameters are independent. Equation 23 exhibits a singular point at $\varphi_\infty = 9$; for $\varphi_\infty \le 9$, the roots of $\boldsymbol{\xi}$ are complex, which have no physical meaning. Hence, systems with parameter values in this range have no physical meaning.

The Reduced BMP Model. The critical point plays an important role because the set of equations can be rewritten in terms of the critical properties or in terms of the model parameters. By definition of the reduced variables, $\sigma_r = \sigma/\sigma_c$, $\dot{\gamma}_r = \dot{\gamma}/\dot{\gamma}_c$, and $\varphi_r = \varphi/\varphi_c$, eq 18 becomes

$$(\varphi_c^{-1} - \varphi_r) + k\dot{\gamma}_c\sigma_c(1 + \vartheta\dot{\gamma}_c\dot{\gamma}_r)(\varphi_c^{-1}\varphi_\infty - \varphi_r)\sigma_r\dot{\gamma}_r = 0 \quad (24)$$

Since the reduced fluidity is not an independent variable, there is only one independent variable in eq 24.

Equations Near the necp and Critical Exponents. At the nonequilibrium critical point, the shear intensity parameter takes the value $\vartheta = \vartheta_c$, and so eq 24 can be solved for the normalized stress. Near the critical point, the binomial expansion yields

$$\sigma_r = -\frac{1}{2k\sigma_c\varphi_\infty\dot{\gamma}_c\dot{\gamma}_r} + \frac{\vartheta_c}{2k\sigma_c\varphi_\infty} + \frac{\varphi_c\dot{\gamma}_r}{2\varphi_\infty} - \frac{\vartheta_c^2\dot{\gamma}_c^2\varphi_c\dot{\gamma}_r^3}{2\varphi_\infty} + \sqrt{\frac{\varphi_c}{\dot{\gamma}_c k\sigma_c\varphi_\infty}} - \sqrt{\frac{\varphi_c}{\dot{\gamma}_c k\sigma_c\varphi_\infty}}\frac{\vartheta_c\dot{\gamma}_c\dot{\gamma}_r}{2} + \sqrt{\frac{\varphi_c}{\dot{\gamma}_c k\sigma_c\varphi_\infty}}\frac{\vartheta_c^2\dot{\gamma}_c^2\dot{\gamma}_r^2}{2} \quad (25)$$

Next, the magnitude of each term in eq 25 was estimated as ϑ was varied. It was found that with the exception of the third, second, and fifth terms, which increase as $\vartheta \to \vartheta_c$, the rest were negligible. The critical isotherm equation is readily obtained

$$\sigma_r = \frac{\vartheta_c^2\dot{\gamma}_c^2\varphi_c}{2\varphi_\infty}\dot{\gamma}_r^3 + \left(\frac{\varphi_c}{2\varphi_\infty} - \sqrt{\frac{\varphi_c}{\dot{\gamma}_c k\sigma_c\varphi_\infty}}\frac{\vartheta_c\dot{\gamma}_c}{2}\right)\dot{\gamma}_r + ... \quad (26)$$

From eq 26 it is evident that the first term of the expansion is the dominant part, and hence, the critical exponent, δ, which relates the reduced shear stress with the reduced shear rate near the critical point, is equal to 3.

Nonequilibrium Phase Equation (Coexistence Line). As shown elsewhere,[9,28] the criterion of the equal areas in the curve of dissipated energy versus shear rate can be used to determine the coexistence stress between the coexisting phases in the shear-banding flow region. The integral that results when the equal-areas criterion is used has no analytical solution. However, because the symmetry of the curve, the shear rate, and the shear stress at the critical point are nearly equal to those at the inflection point of the flow curve, then $\dot{\gamma}_c \approx \dot{\gamma}_I$ and $\sigma_c \approx \sigma_I$. These approximations lead to analytical expressions at the inflection point by setting the second derivative to zero in eq 18. The first derivative at $\dot{\gamma}_I$ is

$$\left.\frac{d\sigma}{d\dot{\gamma}}\right|_{\dot{\gamma}_I} = \frac{b_1 + a_1\vartheta}{b_2 + a_2\vartheta} \quad (27)$$

where

$$a_1 = (-3\sigma_I\dot{\gamma}_I^2 + 2\dot{\gamma}_I\varphi_\infty\sigma_I^2) \qquad b_1 = \varphi_\infty\sigma_I^2 - 2\sigma_I\dot{\gamma}_I - \frac{1}{k}$$

$$a_2 = (-2\varphi_\infty\sigma_I\dot{\gamma}_I^2 + \dot{\gamma}_I^3) \qquad b_2 = -2\varphi_\infty\sigma_I\dot{\gamma}_I + \dot{\gamma}_I^2 - \frac{1}{k}$$

The second derivative given below is equal to zero at the inflection point, i.e.

$$\frac{d^2\sigma}{d\dot{\gamma}^2} = -\frac{\frac{d\sigma}{d\dot{\gamma}}\left[-\frac{\varphi_\infty}{\vartheta}2\left(\sigma + \dot{\gamma}\frac{d\sigma}{d\dot{\gamma}}\right) - \varphi_\infty 2\left(\sigma 2\dot{\gamma} + \dot{\gamma}^2\frac{d\sigma}{d\dot{\gamma}}\right) + \frac{2\dot{\gamma}}{\vartheta} + 3\dot{\gamma}^2\right]}{\left[-\frac{1}{k\vartheta} - \frac{\varphi_\infty}{\vartheta}2\sigma\dot{\gamma} - \varphi_\infty 2\sigma\dot{\gamma}^2 + \frac{\dot{\gamma}^2}{\vartheta} + \dot{\gamma}^3\right]}$$
$$\left(\varphi_\infty\sigma^2 - \frac{\sigma}{\vartheta}\right)2 - 3\sigma 2\dot{\gamma} + \frac{\left[\frac{\varphi_\infty}{\vartheta}2\sigma + \left(\varphi_\infty 2\sigma - \frac{1}{\vartheta}\right)2\dot{\gamma} - 3\dot{\gamma}^2\right]\frac{d\sigma}{d\dot{\gamma}}}{\left[-\frac{1}{k\vartheta} - \frac{\varphi_\infty}{\vartheta}2\sigma\dot{\gamma} - \varphi_\infty 2\sigma\dot{\gamma}^2 + \frac{\dot{\gamma}^2}{\vartheta} + \dot{\gamma}^3\right]} = 0 \tag{28}$$

After substituting eq 27 into eq 28 and up to first-order terms in $\dot{\gamma}$, the plateau stress can be determined, yielding

$$\sigma_P = \sigma_c + \left(\frac{2\dot{\gamma} + 3\vartheta\dot{\gamma}^2}{1 + 3\vartheta\dot{\gamma}}\right)\frac{b_1 + a_1\vartheta}{b_2 + a_2\vartheta} \tag{29}$$

where σ_c is the critical stress given in eq 21.

The two remaining roots are $(\dot{\gamma}_I + a)$ and $(\dot{\gamma}_I - a)$, which can be determined as follows

$$(\dot{\gamma} - \dot{\gamma}_I)(\dot{\gamma} - \dot{\gamma}_I - a)(\dot{\gamma} - \dot{\gamma}_I + a) = 0 \tag{30}$$

Solving for a produces

$$\left(\left(\frac{\vartheta\varphi_\infty\sigma_I - 1}{3\vartheta}\right)^2 - \frac{3}{k(\vartheta\varphi_\infty\sigma_I)}\right)^{1/2} = a \tag{31}$$

The coexistence curve is defined as $\dot{\gamma}_{c1} - \dot{\gamma}_{c2} = (\dot{\gamma} - \dot{\gamma}_I - a) - (\dot{\gamma} - \dot{\gamma}_I + a) = 2a$, and therefore

$$\dot{\gamma}_{c1} - \dot{\gamma}_{c2} = 2\left(\dot{\gamma}_I^2 - \frac{1}{k\vartheta\dot{\gamma}_I}\right)^{1/2} \tag{32}$$

The critical exponent β cannot be obtained analytically from eq 32, and so it has to be estimated numerically from the slope as $\vartheta \to \vartheta_c$ (see Figure 1), yielding an approximate value of 5.725 87.

Similarly to and in analogy with the isothermal compressibility, the isothermal flow susceptibility is defined here as

$$\kappa_T = -\frac{1}{\dot{\gamma}}\left(\frac{d\dot{\gamma}}{d\sigma}\right)_T \tag{33}$$

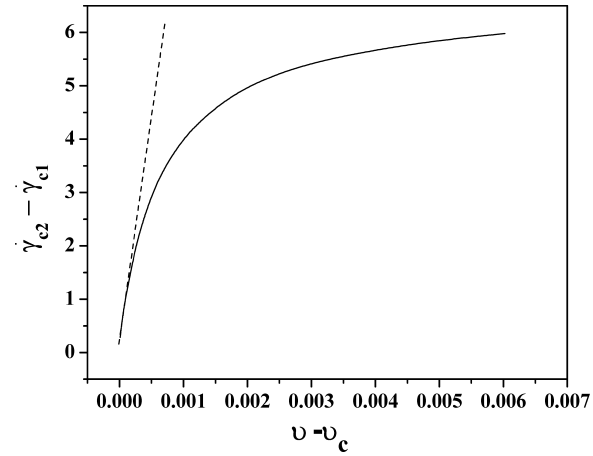

Figure 1. Difference of normalized critical shear rates versus difference of normalized shear-banding intensity parameter.

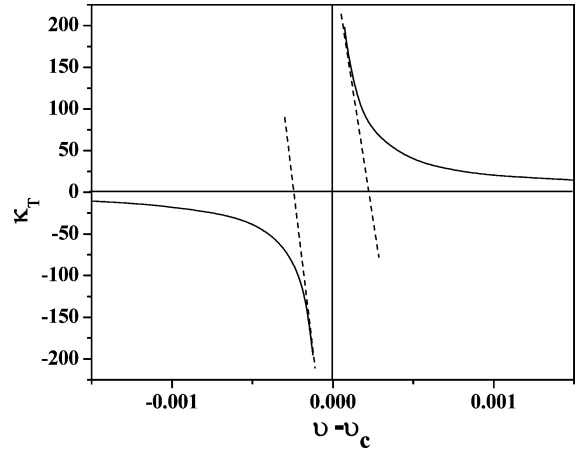

Figure 2. Isothermal flow susceptibility versus $\vartheta - \vartheta_c$.

From eq 18 it is obtained that

$$\kappa_T = -\frac{1}{\dot{\gamma}}\left(\frac{d\dot{\gamma}}{d\sigma}\right)_T = -\frac{\left(\frac{\varphi_\infty}{\vartheta} - \frac{1}{k\vartheta\sigma^2}\right) + \varphi_\infty\dot{\gamma}}{\frac{1}{3}\left(-\frac{\varphi_\infty}{\vartheta}\sigma + \frac{1}{k\vartheta\sigma}\right) + \left(-\varphi_\infty\sigma + \frac{1}{\vartheta}\right)\frac{2}{3}\dot{\gamma} + \dot{\gamma}^2} \tag{34}$$

This expression diverges at the critical point, and the critical exponent ν tends to 11.5. Notice that $\nu \approx 2\beta$. Again this exponent is estimated numerically from the slope as $\vartheta \to \vartheta_c$ (see Figure 2). Here it is evident that this function diverges as the nonequilibrium critical point is approached, similar to the divergence of the equilibrium counterpart property, the thermal compressibility as the critical point is approached.

In addition and in analogy to the heat capacity at equilibrium C_x, where x can be P or V, the normalized power dissipation under shear-banding flow is defined here as

$$C_\varepsilon = \frac{G_0\varphi}{N}\left(\frac{\partial\sigma_r\dot{\gamma}_r}{\partial\vartheta}\right)_\varepsilon \tag{35}$$

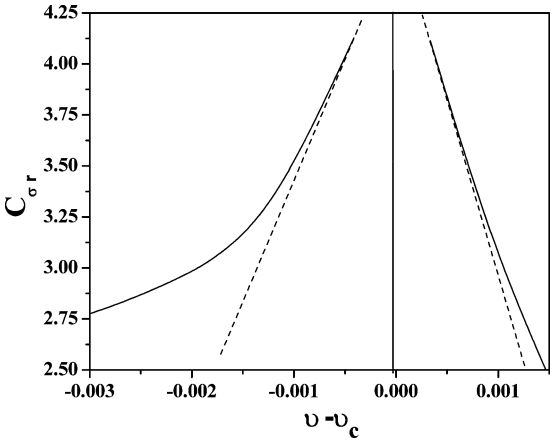

Figure 3. Normalized power dissipation under shear-banding flow versus $\vartheta - \vartheta_c$.

where the subindex ε can be σ_r or $\dot{\gamma}_r$ and ϑ may depend on temperature, surfactant concentration, or the surfactant-to-additive concentration ratio. N is the mass of the system. Performing the derivative indicated in eq 35 and using eq 27, near the critical point it is obtained that

$$C_{\sigma_r} = -\frac{1}{N}\frac{3 + k^{1/3}\vartheta^{-2/3} - \varphi_\infty}{k\sigma_c\varphi_\infty(3 + k^{1/3}\vartheta^{-2/3} - 1)}\frac{1}{(1 + \vartheta\dot{\gamma}_c)^2} \qquad (36)$$

As it is shown in Figure 3, this function diverges as the necp is approached. The critical exponent α was determined numerically from the slope as $\vartheta \rightarrow \vartheta_c$ (see Figure 3), and it tends to 2.2.

Widom's and Rushbroke's Inequalities and the Physical Meaning of Critical Exponents. The three critical exponents follow the extended Widom's relationship inasmuch as $\nu \geq \beta(\delta - 1)$, i.e., $2\beta \geq \beta(3 - 1)$, and the extended Rushbroke's relationship since $\alpha + 2\beta - \nu \geq 2$, i.e., $2.2 + 2\beta - 2\beta \geq 2$. Although the critical exponents for BMP fluid are nonclassic and take unusual values, the scaling hypothesis for nonequilibrium systems holds since these critical exponents still follow the extended Widom's relationship and the Rushbroke's inequality.[30,31]

Results and Discussion

Figure 4 depicts the dimensionless shear stress (σ/G_0) as a function of dimensionless shear rate ($\dot{\gamma}\,\tau_R$) for decreasing values of the reduced shear-banding intensity parameter ϑ using eq 18. The same data are plotted in the usual way (σ versus $\dot{\gamma}$) in the inset. In order to produce more *realistic* predictions, experimental parameters of the BMP model ($k\lambda$, φ_0, φ_∞, and G_0) for a 5% CTAT aqueous solution (reported in Table 1) were used.[8] When the data is plotted as σ against $\dot{\gamma}$, there are individual flow curves for each value of the shear-banding intensity parameter without overlapping among the curves (see inset). However, the dimensionless BMP model predicts that all data collapse in a single line for $\dot{\gamma}\,\tau_R < 1$, similarly to experimental data reported in the literature.[20,26,29] The shear-banding region width, which is equal to $\dot{\gamma}_{c1} - \dot{\gamma}_{c2}$, diminishes with decreasing ϑ (this is equivalent to increasing isotherms) up to a value at which the stress plateau disappears and an inflection is noticed. The similarity of this plot with the van der Waals pressure−density isotherm phase diagram is remarkable. The dissipated (or extended Gibbs free) energy, as

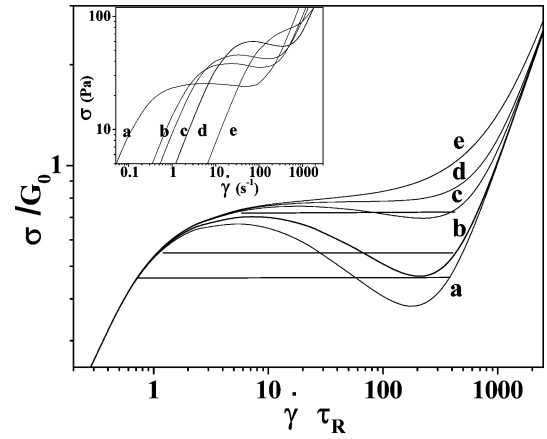

Figure 4. Normalized stress versus normalized shear rate for various normalized shear-banding intensity parameters: (a) 0.015, (b) 0.012, (c) 0.0101, (d) 0.007, and (e) 0.001 (see Table 1). Inset: stress versus shear rate for various normalized shear-banding intensity parameters.

TABLE 1: BMP Model Parameters of the CTAT 5% Weight

T (K)	φ_0	φ_∞	$k\lambda$	ϑ	G_0	τ_R
30	0.0101	7.00	0.0002	0.015	54.5	1.99
38	0.069	10.0	0.00005	0.012	57.5	0.241
40	0.105	11.0	0.00003	0.0101	64.0	0.161
45	0.24	16.0	0.00001	0.007	68.0	0.0517
50	0.45	17.0	0.000009	0.004	68.0	0.0356
55	1.3	19.0	0.000007	0.001	69.0	0.0253

discussed elsewhere,[9,28] depicts a single minimum in the low- and high-shear-rate Newtonian regions (homogeneous flow) and two minima in the multivalued $\sigma-\dot{\gamma}$ region (nonhomogeneous flow). In the latter region, two situations arise: (1) the metastable region, in which one of the minima is deeper than the other, indicating the shear-rate location of the stable state, and (2) the shear-banding region, in which both minima have the same depth. The latter scenario clearly determines the values of the stress plateau and of the critical shear rates for shear banding $\dot{\gamma}_{c1}$ and $\dot{\gamma}_{c2}$. Additionally, at the stress plateau, the amount of each band is determined by the lever rule, similar to equilibrium phase coexistence.

The "reduced dynamic phase diagram" obtained from eq 24 is shown in Figure 5. The diagram is quite similar to that depicted in Figure 4 except that the critical point (or critical line for a two-component system) now has coordinates (1, 1).

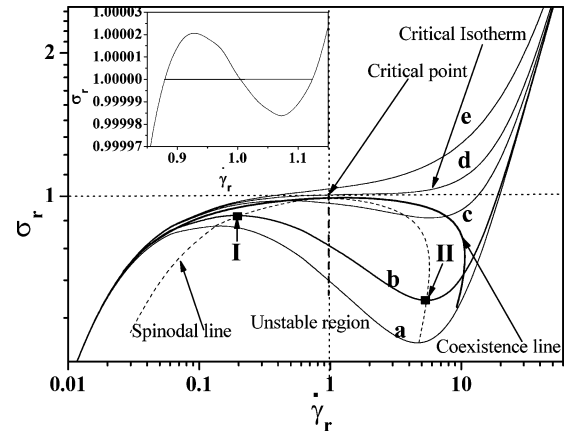

Figure 5. Reduced shear stress versus reduced shear rate for various normalized shear-banding intensity parameters. Inset: enlargement of the values of ϑ close to necp. $\vartheta_c = 0.007\,43$. In the inset, the region near the critical point is enlarged.

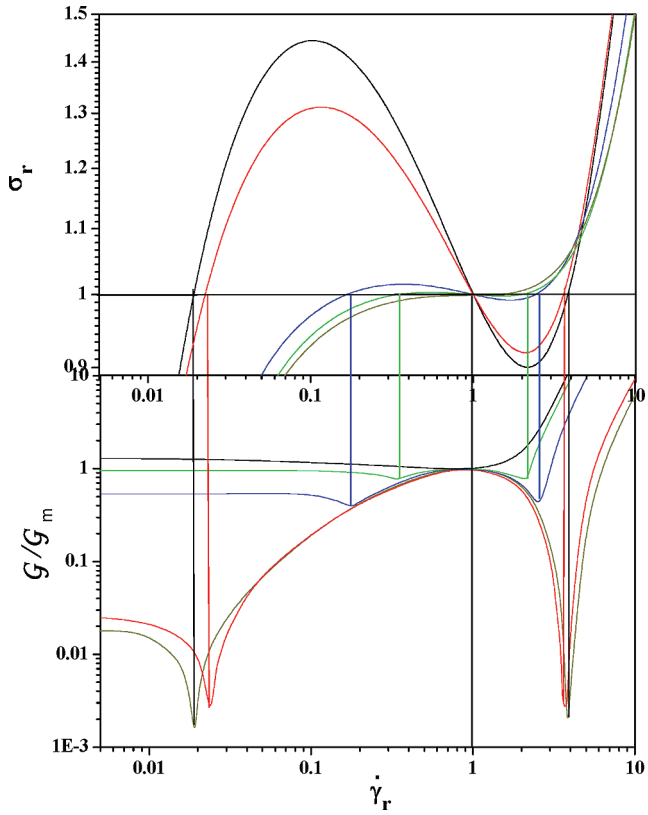

Figure 6. Reduced stress and the normalized dissipated energy ($\mathscr{G}/\mathscr{G}_m$) versus the reduced shear rate for decreasing values of ϑ, after neglecting normal stresses.

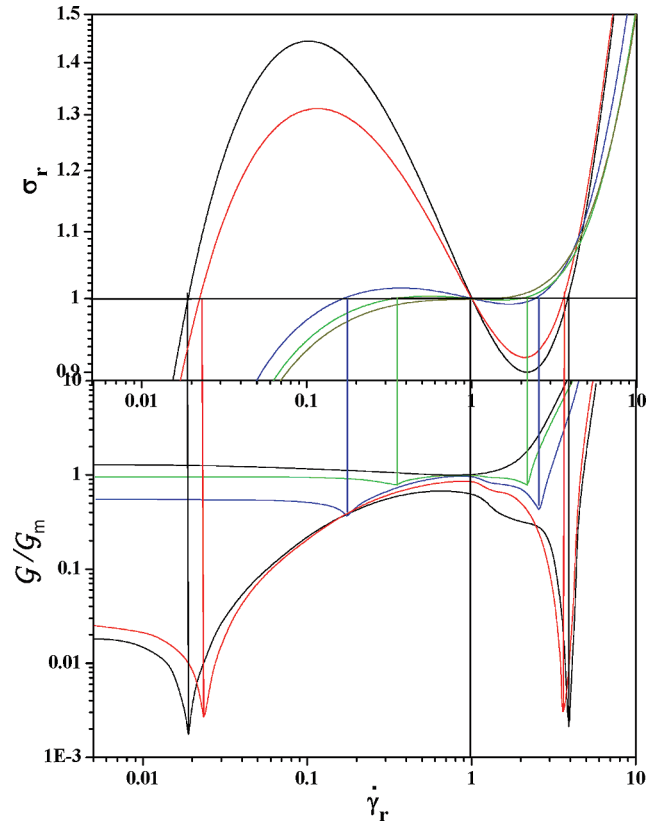

Figure 7. Reduced stress and the normalized dissipated energy ($\mathscr{G}/\mathscr{G}_m$) versus the reduced shear rate for decreasing values of ϑ, where the normal stresses are taken in account.

Notice that in this diagram there are spinodal and coexistence regions that end at a nonequilibrium critical point (necp). Beyond this point (actually it is a line since micellar solutions are at least two-component—water and surfactant—systems), the relation $\sigma-\dot{\gamma}$ becomes monotonic. However, in contrast to the van der Waals equation of state, eq 24 is not universal since there is one nonreduced parameter. The value of ϑ corresponding to the critical isotherm, which describes the curve that passes at the necp, is 0.007 43 for the parameters used in the calculation. Although the curves are not symmetrical, a change of scale from log−log to linear reveals that the curves are indeed symmetrical near the necp. This symmetry is depicted in the inset of Figure 5, where an enlargement around the inflection point is shown for only one curve predicted with a value of the shear-banding intensity parameter ϑ near the necp.

As shown elsewhere (Bautista et al., 2002; 2007), the dissipated or extended Gibbs free energy $\mathscr{G}$ of a fluid system of volume V subjected to a simple shear flow under isothermal−isobaric conditions is given by

$$\mathrm{d}\mathscr{G} = v\lambda_\sigma\left(\frac{4\dot{\gamma}^3}{\varphi^3 G_0^2} + \frac{\dot{\gamma}}{\varphi}\right)\mathrm{d}\dot{\gamma} \qquad (37)$$

where v is the specific volume and φ is the solution of eq 18; the first term within the parentheses of the rhs in eq 37 represents the contribution of the normal stresses, whereas the second term arises from the shear stress.

Figure 6 shows plots of the reduced stress and the normalized dissipated energy ($\mathscr{G}/\mathscr{G}_m$) versus the reduced shear rate for decreasing values of ϑ after neglecting normal stresses, i.e., making $4\dot{\gamma}^3/(\varphi^3 G_0^2) = 0$. The dissipated energy was normalized by the dissipated energy value at the local maximum ($\mathscr{G}_m$) of each curve; this was done to be able to include all the curves in this plot. As discussed above, the dissipated energy curve depicts two minima of equal depth that indicate the position of the stress plateau and the values of the critical shear rates, $\dot{\gamma}_{c1}$ and $\dot{\gamma}_{c2}$. This figure also reveals that the depths of the minima become shallower and that they disappear at the necp giving origin to a flat dissipated energy profile. This is remarkably similar to the behavior of the plots of the Gibbs free energy versus density as the isotherms approach the critical one.[21]

When normal stresses are taken in account, the dissipated energy near the maximum is lower than that calculated in the absence of normal stresses (Figure 7); in addition, the curve exhibits a shoulder at shear rates close to the second minima. However, near the critical point the influence of the normal stresses tends to disappear. In fact, the positions of the stress plateau and $\dot{\gamma}_{c1}$ and $\dot{\gamma}_{c2}$ are practically the same, and they still obey the modified equal-area criterion. Hence, the isothermal susceptibility, the normalized power dissipation, and the critical exponents remain unaltered.

Figure 8 depicts a coexistence line $\sigma_{Plateau}$ versus $(\vartheta - \vartheta_c)$ following a constant shear-rate path that ends at the necp, as indicated by dashed line across the sigmoid flow curve depicted in Figure 5. This plot is equivalent to a $P-T$ plot following an isochoric path that approaches the critical point. For each point selected in the path, there is a correspondent dissipated energy versus shear-rate plot (Figure 8A). Far from the critical point (flow curves a and b in Figure 5), two well-defined minima of equal depth are observed, the positions of which determine the values of $\dot{\gamma}_{c1}$ and $\dot{\gamma}_{c2}$. As the path approximates the necp (curves c and d in Figure 5), the minima become shallower and they approach each other, indicating the shrinking of the stress plateau

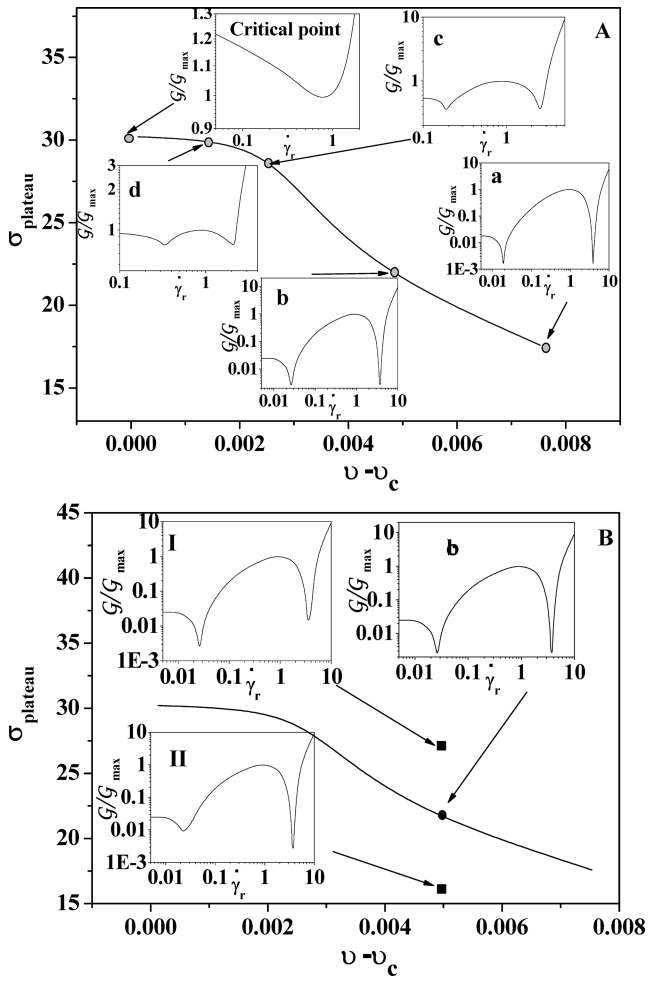

Figure 8. (A) Coexistence line, $\sigma_{\mathbf{r}\,\mathrm{Plateau}}$ versus $\vartheta - \vartheta_c$. Insets: normalized dissipated energy ($\mathcal{G}/\mathcal{G}_m$) versus the reduced shear rate at the conditions of the points on the curve $\sigma_{\mathrm{Plateau}} - (\vartheta - \vartheta_c)$. (B) Coexistence line, $\sigma_{\mathbf{r}\,\mathrm{Plateau}}$ versus $\vartheta - \vartheta_c$. Insets: normalized dissipated energy ($\mathcal{G}/\mathcal{G}_m$) versus the reduced shear rate at the conditions of the points c and the maximum and minimum of the curve $\sigma_\rho - \dot{\gamma}_r$.

until it vanished at the necp. This is similar to the behavior of the Gibbs free energy alone $P-T$ plots following an isochoric path that approaches the critical point. On the other hand, when the stress is above or below the plateau stress within the low- or high-shear-rate metastable regions (see full squares in curve b of Figure 5), the dissipated energy exhibits two minima of different depths at the low- and the high-shear-rate sides of the sigmoid (Figure 8B); in this situation, the lowest minimum corresponds to the metastable state. Notice that in one case the lowest minimum corresponds to the low-shear-rate side (inset I), whereas in the other it corresponds to the high-shear-rate side (inset II) of the sigmoid $\sigma-\dot{\gamma}$ constitutive curve. Hence, the existence of the metastable branches is evident from the analysis presented here. The calculations shown in Figure 8B indicate that a local free energy minimum exists at both branches. Hence, if either of these branches is reached by, for example, controlled-stress measurements, the local free energy minimum guarantees its existence until large enough fluctuations shift the system to the overall minimum within the shear-banding region, and, as a consequence, two bands will form, whose proportions are determined by the lever rule.

Conclusions

In this paper, the BMP model is used to analyze the dynamic equilibrium (steady-state) flow of micellar solutions that exhibit shear banding. The dimensionless version of the model, written in terms of the dimensionless variables, $\hat{\sigma} = \sigma/G_0$, $\hat{\dot{\gamma}} = \dot{\gamma}\,\tau_R$, and $\hat{t} = t/\tau_R$, predicts the *master dynamic phase diagram* proposed by Berret et al.[29] By using an approach analogous to equilibrium critical phenomena theory and defining $\phi = \dot{\gamma}(y) - \dot{\gamma}_{c1}(y)$ as the order parameter of the system, the model reduces to eq 24, written in terms of three reduced variables (σ_r, $\dot{\gamma}_r$, and ϑ) and an independent parameter (k); in this equation, ϑ plays the role of the reduced temperature or reduced concentration. This reduced equation predicts the existence of a critical line and spinodal and coexistence regions, which merge at the nonequilibrium critical line. Further analysis demonstrates that the critical exponents of the coexistence region bounded by $\dot{\gamma}_{c1} - \dot{\gamma}_{c2}$ of the isothermal susceptibility (analogous to the isothermal compressibility) and of the normalized power dissipation under shear-banding flow (analogous to the equilibrium heat capacity) follow Widom's rule and Rushbroke's relationship, but they are nonclassic.

It is noteworthy that the numerical solution of the whole set of eqs 1−3 in which the coupling coefficients are nonzero predicts shear bands, rheo-chaos, and a rich rheological behavior as well as the divergence of the banding interface as the necp is approached.[35] In addition, as mentioned, when the flow−concentration coupling is considered to be first order, instabilities along the gradient and vorticity axes are predicted, allowing the analysis of the dynamic structure factor in the plane of shear.[36]

Finally, and to our knowledge, this is the first time that the shear-banding flow of micellar solutions is examined in light of a critical phenomena theory without adding ad hoc terms. In the second part of this series, experimental evidence that supports this report is presented.

Acknowledgment. We are thankful for the financial support given by CONACYT (The National Council for Science and Technology) through the project 100195.

References and Notes

(1) Onuki, A. *Phase Transitions Dynamics*; Cambridge University Press: New York, 2002.
(2) Onuki, A. *J. Phys.: Condens. Matter* **1997**, *9*, 6119.
(3) Grand, C.; Arrault, J.; Cates, M. E. *J. Phys. II* **1996**, *7*, 1071.
(4) Decruppe, J.-P.; Cappelare, E.; Cresseley, R. *J. Phys. II* **1997**, *7*, 257.
(5) Berret, J.-F. *Langmuir* **1997**, *13*, 2227.
(6) Fischer, P.; Rehage, H. *Rheol. Acta* **1997**, *36*, 13.
(7) Berret, J.-F.; Porte, G. *Phys. Rev. E* **1999**, *60*, 4268.
(8) Soltero, J. F. A.; Bautista, F.; Puig, J. E.; Manero, O. *Langmuir* **1999**, *15*, 1604.
(9) Bautista, F.; Soltero, J. F. A.; Manero, O.; Puig, J. E. *J Phys. Chem. B* **2002**, *106*, 13018.
(10) Criado-Sancho, M.; Casas-Vazquez, J.; Jou, D. *Phys. Rev. E* **1997**, *56* (2), 1887.
(11) Criado-Sancho, M.; Jou, D.; Casas-Vazquez, J.; del Castillo, L. F. *Physica A* **2002**, *30* (1−2), 1.
(12) García-Sancho, M.; Jou, D.; Casas-Vazquez, J.; del Castillo, L. F. *Phys. Rev. E* **2002**, *66* (6), 061803.
(13) Porte, J.; Berret, J.-F.; Harden, J. L. *J. Phys. II* **1997**, *7*, 459.
(14) Olmsted, P. D.; Lu, C.-Y. D. *Phys. Rev. E.* **1999**, *60*, 4397.
(15) Fielding; Omlsted, *Phys. Rev. E* **2003**, *68* (3), 036312, part 2.
(16) Fielding; Omlsted, *Phys. Rev. Lett.* **2003**, *90* (22), 224501.
(17) Fielding, S. M.; Olmsted, P. D. *Eur. Phys. J. E* **2003**, *11*, 65.
(18) Berret, J.-F. In *Molecular Gels. Materials with Self-Assembled Fibrillar Networks*; Weiss, R. G., Terech, P., Eds.; Springer: Secaucus, NJ, 2006.
(19) Puig, J.E.;. Bautista, F. Soltero J. F. A.; Manero O. In *Giant Micelles: Properties and Applications*; Zana, R., Kaler, E. W., Eds.; Francis and Taylor: New York, 2007.
(20) Fernández, V. V. A.; Tepale, N.; Álvarez, J. G.; Pérez-López, J. H.; Macías, E. R.; Bautista, F.; Pignon, F.; Rharbi, Y.; Gámez-Corrales, R.; Manero, O.; Puig, J. E.; Soltero, J. F. A. *J. Colloid Interface Sci.* **2009**, *336*, 842.
(21) Fisher, E.; Callaghan, P. T. *Europhys. Lett.* **2000**, *50*, 803.

(22) Liberatore, M. W.; Nettesheim, F.; Wagner, N. J.; Porcar, L. *Phys. Rev. E* **2006**, *73*, 020504(R).
(23) Johnson, M.; Segalman, D. *J. Non-Newtonian Fluid Mech.* **1977**, *2*, 255.
(24) Spenley, N. A.; Cates, M. E.; McLeish, T. C. B. *Phys. Rev. Lett.* **1993**, *71*, 939.
(25) Bautista, F.; Soltero, J. F. A.; Pérez-López, J. H.; Puig, J. E.; Manero, O. *J. Non-Newtonian Fluid Mech.* **2000**, *94*, 57.
(26) Escalante, J. I.; Macías, E. R.; Bautista, F.; Pérez-López, J. H.; Soltero, J. F. A.; Puig, J. E.; Manero, O. *Langmuir* **2003**, *19*, 6620.
(27) Sandler, S. I. *Chemical and Engineering Thermodynamics*; Wiley: New York, 1989.
(28) Bautista, F.; García, J. P.; Pérez, J. H.; Puig, J. E.; Manero, O. *J. Non-Newtonian Fluid Mech.* **2007**, *144*, 160.
(29) Berret, J.-F.; Porte, G.; Decruppe, J.-P. *Phys. Rev. E.* **1997**, *55*, 1668.
(30) Gunton, J. D.; San Miguel, M.; Sahni, P. S. In *Phase Transitions and Critical Phenomena*; Domb, C., Lebowitz, J. L., Eds.; Academic: New York, 1983; Vol. 8.
(31) Binney, J. J.; Dowrick, N. J.; Fisher A. J.; Newman, M. E. J. *The Theory of Critical Phenomena: An Introduction to the Renormalization Group*; Claredon Press: Oxford, 1993.
(32) Lee, B. P.; Cardy, J. L. *Phys. Rev. E* **1993**, *48*, 2452.
(33) Jou, D.; Casas-Vázquez, J.; Criado-Sancho, M. *Thermodynamics of Fluids Under Flow*; Springer-Verlag: Berlin, 2000.
(34) Manero, O.; Pérez, J. H.; Escalante, J. I.; Puig, J. E.; Bautista, F. *J. Non-Newtonian Fluid Mech.* **2007**, *146*, 22.
(35) García-Sandoval, J. P.; Bautista, F.; Puig, J. E.; Manero, O. *J. Non-Newtonian Fluid Mech.* **2009**, to be submitted.
(36) García-Rojas, B.; Bautista, F.; Puig, J. E.; Manero, O. *Phys. Rev. E* **2009**, *80*, 036313.
(37) Pearson, J. R. A. *J. Rheol.* **2004**, *38*, 309.
(38) Goveas, J. L.; Olmsted, P. D. *Eur. Phys. J. E* **2001**, *6*, 79.
(39) Olmsted, P. D. *Rheol. Acta* **2008**, *47*, 283.
(40) Yuan, X. F.; Jupp, J. G. *Europhys. Lett.* **2002**, *60*, 691.
(41) Yuan, X. F. *Europhys. Lett.* **1999**, *46*, 542.
(42) Spenley, N. A.; Yuan, X. F.; Cates, M. E. *J. Phys. II* **1996**, *6*, 551.
(43) Olmsted, P. D.; Radulescu, O.; Lu, C.-Y. D. *J. Rheol.* **2000**, *44*, 257.
(44) Dhont, J. K. G. *Phys. Rev. E* **1999**, *60*, 4534.

JP906310K